Circumventing Velocity Uncertainty in Imaging Complex Structures

Oz Yilmaz, Anatolian Geophysical and GeoTomo LLC

Summary

In areas with complex near-surface with irregular topography and structurally complex subsurface, there is much uncertainty in rms velocity estimation for prestack time migration, whereas interval velocity estimation for prestack depth migration is despairingly challenging. We often attribute the velocity uncertainty to various factors, including strong lateral velocity variations, heterogeneity, anisotropy, and three-dimensional behavior of complex structures. Nevertheless, it is not easy to identify the cause of and account for the ucertainty as it often is a combination of the various factors. And the analyst struggles with much difficulty when estimating a velocity field whether it is for prestack time or depth migration.

Velocity uncertainty invariably gives rise to erroneously high or low migration velocities, which then causes *two* problems with prestack migration: (1) we fail to *preserve reflector amplitudes*, and (2) we also fail to *position the reflectors* correctly and *focus diffractions to their apexes*. We may choose to solve both problems *simultaneously* or *one after the other*. The quality of image-gathers associated with prestack migration may or may not warrant the simultaneous solution. In areas with irregular topography, complex near-surface, and complex subsurface, it may not. What then? I propose a workflow, applicable to both 2-D and 3-D seismic data, to solve the two problems with prestack time migration one after the other, which includes construction of a zero-offset wavefield to capture and preserve all reflections and diffractions, followed by zero-offset time migration.

The workflow includes construction of an image volume by prestack time migration of shot gathers using a range of constant velocities. This image volume can be used to pick rms velocities for prestack time migration. Yet, the multiplicity of semblance peaks associated with the image volume remains to be perilous. We can sum the image panels within the image volume over the velocity axis to obtain a composite image in time so as to *preserve* all events in the image volume and avoid committing ourselves inadverdently to a velocity field which most likely would have some uncertainty. This summation strategy, however, works if the events within the volume are stationary in time and space. To meet this requirement, we unmigrate each of the image panels within the image volume and then sum over the velocity axis. The resulting unmigrated section actually is equivalent to a zero-offset wavefield. The final step in the workflow is poststack time migration of the zero-offset wavefield. I shall demonstrate this workflow using a field data set from a thrust belt.

Introduction

Figure 1 shows an image section obtained by prestack time migration (PSTM) using an rms velocity field that was constructed by velocity picking from the image volume obtained by PSTM of shot gathers using a range constant velocities from a floating datum. The semblance spectrum at location A exhibits distinctive set of peaks that allows picking a velocity function unambiguously (Figure 2a), whereas the semblance spectrum at location B exhibits a multiplicity of peaks that would give rise to uncertainty in velocity picking (Figure 2b). The stuctural complexity at the central portion of the line observed in Figure 1 is indicative of the difficulties in velocity picking. A further evidence of the troubling nature of velocity uncertainty is provided by the common-image-point (CIP) gathers associated with the PSTM. The CIP gather at location A (Figure 2c) exhibits flat events that confirm the accuracy of the rms velocity field used for PSTM, whereas the CIP gather at location B (Figure 2d) exhibits highly complex and interfering events --- again indicative of the velocity uncertainty within the structurally complex portion of the line. This CIP gather not only is a manifestation of the structural complexity resulting in a poor image (Figure 1), but also is practically unusable for velocity update based on flatness of events, nor can it be used for verification of the accuracy of the rms velocity field used for PSTM.

This leads us to the following question: Can we *circumvent* the velocity unccertainty rather than hopelessly struggle to *eliminate* it and produce an image in time better than obtained by conventional PSTM? I present a workflow that provides an answer to this question in the positive.

Back to the Future: Return of the DMO

In the presence of conflicting dips with different stacking velocities, conventional CMP stack is not equivalent to a zero-offset wavefield. Within the context of subsurface imaging in time, this is the compelling reason for doing prestack time migration in lieu of poststack time migration, aside from the fact that the former also is used for rms velocity estimation and updating based on the flatness of events in CIP gathers. Prior to the age of PSTM, a workflow for time migration developed in the 1980s included dip-moveout (DMO) correction to correct for the dip and source-receiver azimuth effects on stacking velocities (Levin, 1971; Sherwood et al., 1978; Yilmaz and Claerbout, 1980; Deregowski, 1982; Hale, 1984; Beasley, 1992; Yilmaz, 2001). With the increase in computational power, this resource-intensive workflow with multiple stages of velocity analysis soon was replaced in the 1990s by the familiar PSTM workflow.

Nevertheless, we can draw a lesson from DMO processing to devise a workflow for PSTM that circumvents velocity uncertainty. The image in time obtained by the DMO workflow essentially is equivalent to the image obtained by PSTM, provided lateral velocity variations are within the bounds of time migration. This statement is symbolically expressed by the following equation:

NMO + DMO + stack + tmig = PSTM,

where *tmig* stands for time migration after stack.

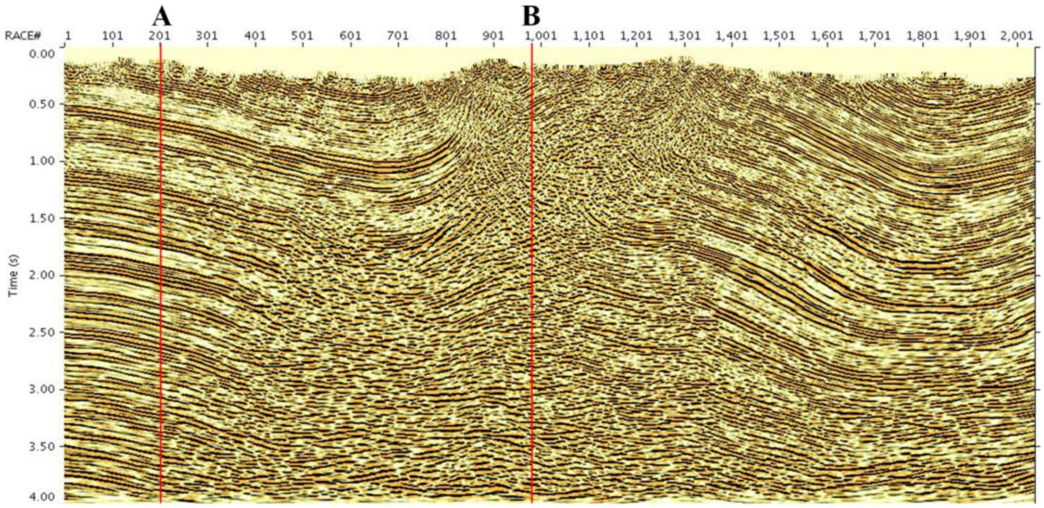

Figure 1. An image section obtained by prestack time migration (PSTM) from a thrust belt. The rms velocity semblance spectra and common-image-point (CIP) gathers at locations A and B are shown in Figure 2.

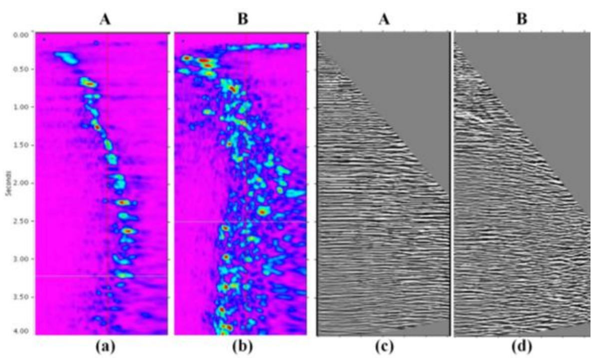

Figure 2. The rms velocity semblance spectra (a) and (b), and CIP gathers (c) and (d) at locations A and B shown in Figure 1.

Add *demig* to both sides of this equation to get:

NMO + DMO + stack + tmig + demig = PSTM + demig,

where *demig* stands for demigration --- in this case, *inverse of tmig*. This means that the terms *tmig* and *demig* on the left-side of the equation cancel each other, and we obtain:

NMO + DMO + stack = PSTM + demig.

Note that the left-side of this equation yields the *zero-offset wavefield*:

zero-offset wavefield = PSTM + demig.

This means that, as an alternative to the DMO workflow, we can obtain the zero-offset wavefield by PSTM followed by demigration of the resulting image. However, this equation implies a commitment to an rms velocity field for PSTM, which may have much uncertainty. I propose the following workflow to construct a zero-offset wavefield without the commitment to an rms velocity field so as to circumvent velocity uncertainty:

(1) Estimate a model for the near-surface by nonlinear traveltime inversion applied to first-arrival times picked from shot gathers and calculate the medium- to long-wavelength shot-receiver statics.

(2) Apply shot-receiver statics and an apropriate single-channel signal processing sequence to shot records. This sequence may include time-variant spectral whitening to account for the signal nonstationarity and flatten the spectrum within the signal passband so as to reduce the strength of the large-amplitude, low-frequency sorface waves; and predictive deconvolution to shape the spectrum to a bell curve that is slightly asymmetric in favor of the low-frequency side of the signal band with its peak coincident with the dominant signal frequency.

(3) Estimate short-wavelength shot-receiver residual statics based on stack-power optimization, and apply them to moveout-corrected CMP gathers.

(4) Now perform the first multichannel signal enhancement in the CMP domain: Radon transform to attenuate coherent linear noise and random noise.

(5) Return to the shot-receiver domain and, if required, perform an additional multichannel signal enhancement to further attenuate coherent linear noise and random noise.

(6) Perform prestack time migration of all shot gathers using a range of constant veelocities and obtain a set of image panels that form an image volume in *(V, X, T)* coordinates, where *V* is the rms velocity, *X* is the midpoint, and *T* is the event time after migration.

(7) Perform a multichannel signal processing to each of the velocity panels *(X, T)* to increase signal coherency.

(8) Demigrate each of the velocity panels using the same constant velocity that was used for PSTM in step 6, and create a zero-offset volume in *(V, X, T)* coordinates, where *V* is the rms velocity, *X* is the midpoint, and *T* is the zero-offset event time before migration. We have preserved in this zero-offset volume all reflections and diffractions that are present in the signal-processed shot gathers. Additionally, each of these demigration panels is essentially a replica of a zero-offset wavefield. As such, events are stationary both in time and space.

(9) Apply Radon transform to each of the velocity gathers in *(V, T)* coordinates to reduce the horizontal smearing of amplitudes associated with finite cable length and discrete sampling along the offset axis.

(10) Using the zero-offset volume with the improved event coherency by multichannel signal processing, sum over the velocity axis to obtain a composite zero-offset wavefield (Figure 3) so as to *preserve all reflections and diffractions* and avoid committing ourselves inadverdently to a velocity field which most likely would have some uncertainty.

(11) Now return to the image volume (step 7) and estimate an rms velocity field that should have lateral velocity variations only within the bounds of time migration.

(12) Perform poststack time migration of the composite zero-offset wavefield from step 10 using the rms velocity field from step 11 (Figure 4). This is the *principal image* in time that can be used for structural interpretation. Compare this image with the image obtained by PSTM shown in Figure 1, and note the significant improvement of the structural complexity in the central portion of the line.

(13) Perform Dix conversion of the rms velocity field from step 11 to obtain an inerval velocity field.

(14) Finally, perform poststack depth migration of the composite zero-offset wavefield from step 10 using the interval velocity field from step 13. This is the *auxiliary image* in depth that can be used for structural interpretation.

I refer to the image in depth as auxiliary, for velocity-depth model estimation in areas with severe lateral velocity variations is perilously time-consuming. More importantly, the estimated velocity-depth model will always have inaccuracies such that the resulting image in depth will not be as useful as the image in time for structural interpretation. I wish to express this underlying philosopy for imaging in time and in depth in areas with severe lateral velocity variations by the following lines:

Kronos gave us the Arrow of Time
So that we may observe Depths of the Earth.
But then, Hades deceived us with the Arrow of Depth
So that we may fall into our Death.

An alternative to the summation described in step 9 over the velocity axis of the zero-offset volume is sumation within a velocity corridor. Based on a weighted summation over the velocity axis, Landa (2013) also proposed a path-integral method to obtain the composite zero-offset wavefield. Application of this method to obtain the time-migrated image from the image volume described in step 6 is proposed by Landa et al. (2006) and its use for migration velocity analysis is suggested by Schleicher and Costa (2009). It is worth to explore in the future the potential use of the path-integral method for improved composite zero-offset wavefield.

Conclusions

The proposed workflow essentially involves a transformation from the observation domain (field records) to the zero-offset domain (the demigration, or zero-offset, volume described in step 8) to preserve reflections and diffractions. Rather than struggling to *eliminate* the uncertainty in velocity estimation for PSTM completely --- an impossible task, the workflow *circumvents* the velocity uncertainty. Because events in the zero-offset volume are stationary both in time and space, we can sum over the velocity axis to obtain a composite zero-offset wavefield so as to preserve all events contained in the volume and avoid committing ourselves inadverdently to a velocity field which most likely would have some uncertainty. The resulting composite zero-offset wavefield can then be migrated by poststack time migration. The resulting image would have all the events, albeit some may be mispositioned because of velocity errors. The poststack time migration, however, can be repeated using a revised rms velocity field to position the events correctly. If, on the other hand, an rms velocity field with much uncertainy is used for PSTM, the resulting image not only would have mispositioned events but also some events with incomplete focusing or missing altogether. To remedy both the problems of event mispositioning, incomplete focusing and missing events, velocity field would have to be updated and PSTM would have to be repated --- a formidably time-consuming and resource-driven exercise, especially in case of 3-D imaging. In contrast, the proposed workflow produces a composite zero-offset wavefield and only requires poststack time migration that can be repated at much less cost.

Acknowledgement

I thank the owner of the field data, who requested to be anonymous, for permission to present the case study.

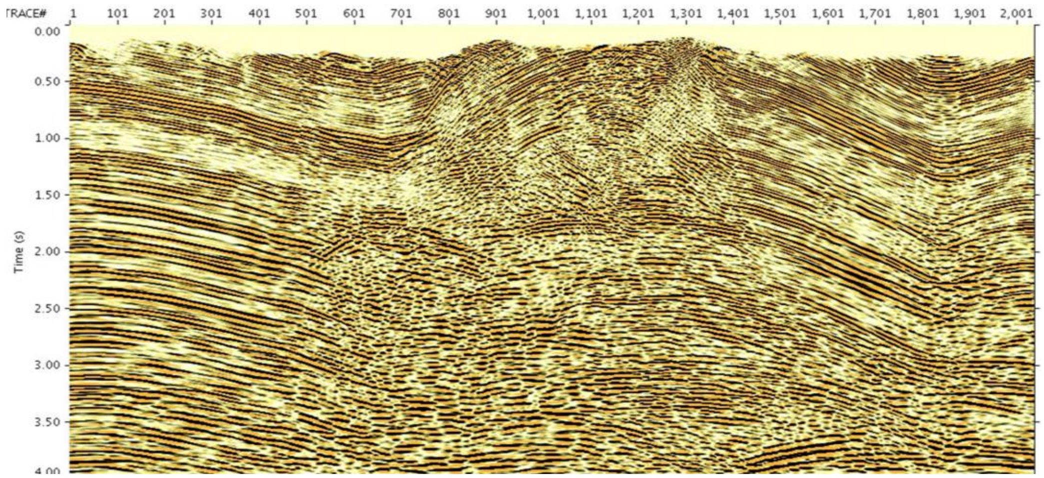

Figure 3. The composite zero-offset wavefield obtained by summation of the demigration panels of the zero-offset volume (step 9 of the workflow described in the text).

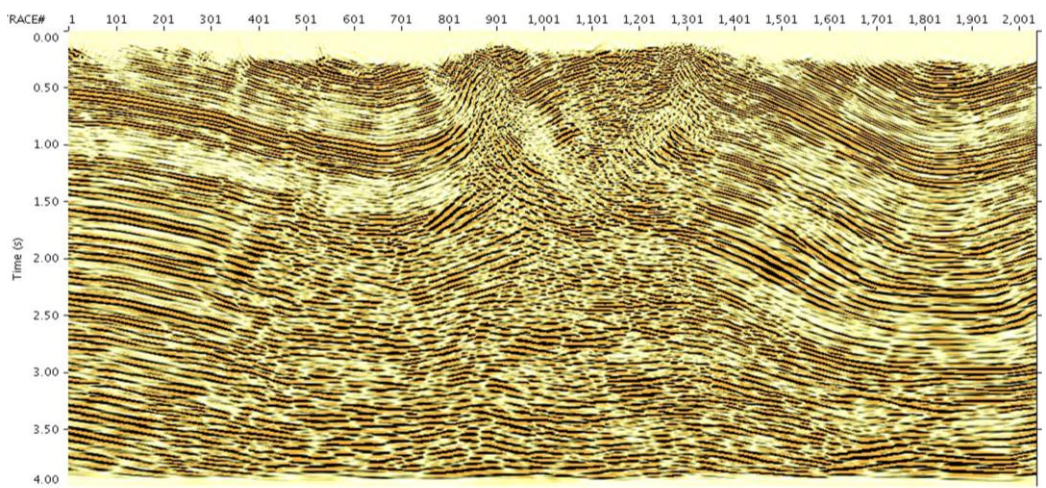

Figure 4. Poststack time migration of the composite zero-offset wavefield shown in Figure 3. This is the *principal image* in time that can be used for structural interpretation. Compare this image with the image obtained by PSTM shown in Figure 1, and note the significant improvement of the structural complexity in the central portion of the line.